Accepted Manuscript

Self-healing ability assessment of irradiated multilayered composites: A continuum approach

Jaime Ortún-Palacios, Antonio Mario Locci, Francesco Delogu, Santiago Cuesta-López

PII: S0022-3115(18)30565-8

DOI: https://doi.org/10.1016/j.jnucmat.2018.10.030

Reference: NUMA 51269

To appear in: *Journal of Nuclear Materials*

Received Date: 25 April 2018

Revised Date: 13 September 2018

Accepted Date: 20 October 2018

Please cite this article as: J. Ortún-Palacios, A.M. Locci, F. Delogu, S. Cuesta-López, Self-healing ability assessment of irradiated multilayered composites: A continuum approach, *Journal of Nuclear Materials* (2018), doi: https://doi.org/10.1016/j.jnucmat.2018.10.030.

Self-healing ability assessment of irradiated multilayered composites: A continuum approach

Jaime Ortún-Palacios[1,2,*], Antonio Mario Locci[3], Francesco Delogu[3], Santiago Cuesta-López[1,2,4]

[1]*International Research Centre in Critical Raw Materials (ICCRAM), University of Burgos, Plaza Misael Bañuelos s/n, 09001 Burgos, Spain*

[2]*Advanced Materials, Nuclear Technology and Applied Bio/Nanotechnology, Consolidated Research Unit UIC-154, Castilla y León, Spain. University of Burgos, Hospital del Rey s/n, 09001 Burgos, Spain*

[3]*Dipartimento di Ingegneria Meccanica, Chimica e dei Materiali, Università degli Studi di Cagliari, Via Marengo 2, 09123 Cagliari, Italy*

[4]*International Center for Advanced Materials and Raw Materials of Castilla y León, ICAMCyL Foundation, 24492 Cubillos del Sil (León), Spain*

**Correspondence should be addressed to*
Jaime Ortún-Palacios; jortun@ubu.es

September 2018

Abstract

Atomistic simulations have revealed an unconventional behavior of point defects at interfaces found in multilayer composites synthesized by physical vapor deposition but the observed mechanisms that involve point-defect annihilation are subject to time-scale limitations. So, a mathematical model that describes long-term evolution of point defects in such materials under irradiation is presented in this work. Firstly, the effect of interface point-defect trapping and recombination mechanisms on point-defect concentrations has been studied. In addition, the effect of interface self-interstitial atoms loading, which has been seen during collision cascades, and constitutional vacancies has been studied too. Two interface configurations have been considered between metals in a β-α-β three-layer system (α = Cu and β = Nb, or V), KS_{min} and KS_1. These interfaces correspond to ground-state and defect-free KS structures respectively. The respond to irradiation of the systems investigated here, Cu/Nb and Cu/V, depends on both, interface characteristics and bulk properties. Nonetheless, the influence of the properties of one metal in the point-defect evolution of the other metal is only effective if there are constitutional vacancies at the interface, i.e., for KS_{min}. Especial attention has been paid to the behavior of the same metal (Cu) when it is surrounded by diverse metals (Nb, or V) with the aim of comparing quantitatively our model predictions with experimental results reported elsewhere. The lower concentration of vacancies in Cu layer of Cu/Nb system at steady state is due to the low mobility of vacancies in niobium.

1. Introduction

Heterophase boundaries are interfaces with a great complexity between crystals of dissimilar chemistry, structure and orientation. The increase of interfacial area respect total volume can make material behavior to be influenced or even determined by above boundaries. Thus, nanoscale metallic multilayer composites (NMMCs) with ultra-high strengths and enhanced radiation damage tolerance could be designed tailoring layer thickness to take advantage of the atomic structure and energetics of the interfaces **[1]**. Nevertheless, the increase of interfaces number is not enough as they must be of the correct type **[2]**. In spite of their well-known importance, it has not been possible to study heterophase boundaries in detail until last years in which the situation has changed thanks to analyses with increased resolution and sensitivity besides to high-performance computational resources **[3]**.

Variations in composition, stress or temperature may cause some interfaces to change easily from a metastable state to another one of almost the same energy which makes them affect a wide variety of processes **[4]**. Kurdjumov–Sachs (KS) **[5]** and Nishiyama–Wassermann (NW) **[6,7]** orientation relations are commonly found in close-packed fcc/bcc interfaces being the former the most studied. Despite their incommensurate character, a quasi-periodic pattern of patches may be present in these interfaces. This is the case of the interface atomic configuration termed KS_1 in Cu/Nb multilayer composites which have been used as model systems. While in KS_1 there are patches of undercoordination, i.e., interface areas where a Cu and Nb atom are practically above each other, no patches of undercoordination exist in KS_2 **[8]**. KS_1 is obtained joining Cu and Nb layers with the KS orientation relation. However, interfacial Cu plane in KS_2 is homogeneously strained and rotated in such a way that makes this interface slightly favorable energetically respect KS_1. As a consequence, KS_2 contains an extra interface between the strained interfacial Cu plane (Cu_α) and the rest of Cu layer, Cu_α/Cu, in addition to Cuα/Nb one.

Lattice mismatch in heterophase interfaces may be accommodated by lattice strain, or by misfit dislocations injection which makes component crystals to return to the unstrained state. The existence of misfit dislocations can be proved by means of a disregistry analysis throughout the interface **[4]**. For such analysis, the relaxed structure and the correct reference state **[9,10]**, in which the interface is coherent, are needed. There are two sets of parallel misfit dislocation in Cu/Nb interface of KS_1 and there is one set in each interface of KS_2 (Cu_α/Nb and Cu_α/Cu). Parameter values characterizing above sets of interfacial dislocations present in KS_1 and KS_2 can be found in **Ref. (4)** while their relative arrangement is illustrated in **Ref. (11)**.

Real Cu/Nb interfaces are not atomically flat even in multilayer composites synthesized by physical vapor deposition (PVD). Shear elastic constants of Cu/Nb interfaces have been demonstrated to be highly temperature dependent and easily influenced by the step density **[12]**. Therefore, interfaces with different atomistic roughnesses may have different shear stiffnesses. Severe plastic deformation (SPD) techniques allow to create Cu/Nb interfaces with different orientation of the habit planes to that of KS_1 and KS_2 **[13]**. This is the case of the interface studied in above work (Cu/Nb_{spd}) and that has been compared with KS_1 and

KS_2 (Cu/Nb_{pvd}). Cu/Nb_{spd} contains three sets of parallel misfit dislocations. The dissimilarities found in the interface shear response of Cu/Nb_{pvd} and Cu/Nb_{spd} do not proceed from the difference of interface energy **[14]** but from the difference in misfit dislocation structure. Just one set of Cu/Nb_{spd} misfit dislocations has a Burgers vector within the interface plane which implies that the interface shears in that direction, i.e., the transverse direction along interface, but not at all in the horizontal direction along interface. The other two sets have Burgers vectors with non-zero component in the direction perpendicular to interface. These misfit dislocations are not able to glide within the interface by themselves, they would need climb to occur. Nevertheless, misfit dislocation climb is unlikely to occur **[13]**.

Light-ion beams are frequently used to study the effects of radiation on materials properties **[15]**. Such bombarding particles provoke atomic displacements that lead to the creation of self-interstitial atoms (SIAs) and vacancies mostly. These defects predominate in a region close to the irradiated surface where ion amount is negligible **[16]** and can be removed by means of recombination. One of the most promising strategies in the mitigation of radiation damage is the introduction of heterophase interfaces with enhanced ability to annihilate point defects **[1]**. An Embedded-Atom-Method (EAM) potential developed from Cu and Nb single-element potentials, and the Ziegler–Biersack–Littmark (ZBL) universal potential were joined to describe the interatomic and short range repulsive interactions respectively in Cu/Nb multilayers composites **[17]**. The resulting potential was used to simulate collision cascades nearby Cu/Nb-KS_1 interface as well as in single Cu and Nb crystals. The number of point defects produced per keV of primary knock-on atom (PKA) energy in Cu/Nb multilayers was 50-70% lower than in single Cu and Nb crystals **[17]**. This unique response of Cu/Nb NMMCs to irradiation arises from the extraordinary behavior of point defects in Cu/Nb interfaces. Indeed, void density and size in Cu layers of Cu/Nb NMMCs decrease when reducing the thickness **[18]**.

Point-defects formation energies in Cu/Nb interfaces and bulk constituent metals were compared with the purpose of evaluating the point-defect trapping capacity of such interfaces. Molecular Dynamics (MD) simulations revealed similar and smaller point-defect formation energies away from Cu/Nb_{pvd} interfaces and close to them respectively. Some Cu SIAs show similar formation energies to interfacial values at distances of up 1 nm **[4]**. The relaxation process analysis of a Cu SIA located 1 nm from Cu/Nb interface showed a spontaneous migration to the interface without any energetic barrier or a very small one. The sites of lowest point-defect formation energies in Cu/Nb_{pvd} interfaces are located in the regions of the quasi-periodic pattern commented previously that in turn coincide with the misfit dislocation intersections (MDIs). A Density Functional Theory (DFT)-based explanation was given in strain terms for vacancies **[19]**. A high corrugation exists in MDIs because a Cu atom is nearly on the top of a Nb atom and they repulse each other. The introduction of a vacancy in these regions decreases the corrugation. The cost reduction of introducing a Cu vacancy is such that it ends up being energetically favorable unlike what happens outside of MDI regions. This means that a lower energy interface, KS_{min}, can be found removing appropriate Cu atoms from KS_1 and KS_2 **[4]**. In addition, González et al. calculated the formation energy of a vacancy in the

second plane of both sides of Cu/Nb interface near MDIs and the migration energy to the interfacial plane. Vacancy formation energies are between bulk and interface values, and vacancy migration energies are lower than in the bulk **[20]**, so a successful vacancy trapping effect of Cu/Nb interface is expected.

A Cu atom removal or insertion in KS_1 does not form compact point defects after relaxation but it changes the atomic volume in an extensive region and the interface reconstruction leads to the creation of 4- and 5-atoms rings in the 3-atom ring network **[4]**. A point defect can be seen as a square edge dislocation loop of atomic dimensions **[4,11]**. If the two edge segments of the dislocation loop glide in contrary directions, a screw segment is created. This would be unfavorable energetically unless a screw dislocation with opposite Burgers vector already exists as in this case. The elimination of the screw segment between edge ones results in a screw dislocation with a jog and a kink pair. Thus, a small patch climbs one atomic plane from Cu/Nb interface converting into KS_2 **[11]**. On the other hand, the insertion or removal of an atom in Cu_α plane of KS_2 provokes the shifting of a small patch from Cu_α/Cu to Cu/Nb interface becoming KS_1.

Away from Cu/Nb_{spd} interfaces, point-defect formation energies are similar to the values obtained in single Cu and Nb crystal as it occurs in Cu/Nb multilayer composites synthesized by PVD, but highly variable in their vicinity for vacancies **[13]**. The sites of lowest point-defect formation energies in Cu/Nb_{spd} are located in MDI regions too. No constitutional vacancies are present in Cu/Nb_{spd} interfaces since all vacancy formation energies are positive. Furthermore, no point-defect delocalization occurs. The penalty energy associated to strained Cu_α plane of KS_2 is compensated with the energy gained by avoiding misfit dislocations from intersecting at the same interface plane (KS_1). Hence, differences in the interaction of Cu/Nb_{spd} and Cu/Nb_{pvd} interfaces with point defects may be caused by the inability of Cu/Nb_{spd} misfit dislocations to shift one atomic plane.

In order to test the influence of thermodynamic properties and interface geometry on the atomic structure as well as on interface point-defect formation energies, EAM interaction potentials were fitted to different values of dilute heats of mixing **[21]** and lattice misfit **[22]** respectively keeping the rest of parameters unchanged. Variation of dilute heats of mixing, and therefore bonding strength, does not affect significantly the atomic structure or Cu vacancy formation energies, but it does affect Cu SIA formation ones. Variation of lattice misfit alters significantly the atomic structure due to changes in the misfit dislocation spacing and the dislocation character. All lattice misfits showed Cu point-defect formation energies lower than bulk values except in one case for vacancies. An increase of low vacancy formation energy sites is usually associated to an increase of MDI density so other semicoherent interfaces could be design to trap point defect effectively.

Cu/Nb_{pvd} interfaces not only act as sinks for point defects, they are catalysts for point-defect recombination too. Kink-jog pairs formed after a Cu atom insertion or removal, have dipolar elastic fields that allow long-range interactions between them. This causes a significant increase of the critical distance for Frenkel-pair recombination compared to Cu single crystal **[11]**. On the contrary, the critical distance for Frenkel pair recombination in the interfacial Nb plane is not increased as markedly as in the Cu one because

Nb point defects remain compact. But, despite this, Frenkel pairs formed in Nb layer can also take advantage of the mechanism that aid rapid point-defect recombination in Cu layer if they migrate to the interfacial Cu plane **[4]**. In addition, the emission of SIAs from the interfaces may play an important role in the annihilation of radiation damage. MD simulations demonstrated that Cu SIAs are loaded in Cu/Nb interfaces during the collision cascades **[23]**. Next, such SIAs interact with the remaining vacancies in Cu layer even if the latter are some planes away from the interface. A SIA is emitted from the interface causing an organized movement of adjacent Cu planes atoms that ends with the annihilation of a vacancy. The creation of low vacancy formation energy sites in Cu layer as a result of SIAs loading confirms the existence of long-range SIA-vacancy interactions. The SIA emission mechanism can be seen both in Cu/Nb_{pvd} and Cu/Nb_{spd} interfaces but it has a greater range of interaction in the last ones.

Point-defect clusters delocalize forming 4- and 5-atoms rings in Cu/Nb_{pvd} interfaces as single SIAs and vacancies **[24]**. Either single point defects or SIA clusters extent along set 1 of misfit dislocations while vacancy clusters extend along set 2. Taking as reference ground-state interface, KS_{min}, point-defect cluster formation energy increases linearly with the number of point defects in the cluster unlike in single Cu crystal. The lack of thermodynamic driving forces for clustering besides the higher configurational entropy of isolated point defects than forming a cluster suggest a tendency of point-defect clusters to divide into smaller ones and occupy different MDIs which may be beneficial due to the reduction of void formation.

MD simulations revealed that delocalized point defects migrate along set 1 of misfit dislocations from a MDI to a neighboring one in Cu/Nb_{pvd} interfaces **[24]**. In between, the delocalized point defect extents and reside on both MDIs at the same time. The transition from delocalized state to extended one and vice versa requires the nucleation of thermal kink pairs at neighboring MDI and between both MDIs respectively. Then, a kink-jog of the delocalized point defect annihilates with a kink-jog of the thermal kink pair permitting the transition between states. Thermal kinks nucleation or annihilation determines the energy barriers in the migration path which are smaller than in the bulk. On the contrary, DFT calculations suggest that vacancies stabilize at MDIs once they get trapped **[19]**. Nevertheless, supercell size limitations do not allow considering delocalized vacancies in the last work. In Cu/Nb_{spd} interfaces, point defects are expected to migrate in a conventional way due to the predominant edge character of the three misfit dislocation sets and the incapacity of point defects to delocalize **[13]**. Formation, migration and dissociation of point-defect clusters in Cu/Nb_{pvd} interfaces are governed by a multistage process with similar mechanisms to single point-defect migration ones **[24]**. Either delocalized point defects or thermal kink pairs can be represented by dislocation segments and, saddle points in the migration path of point defects correspond to dislocation nucleation or annihilation. Hence, minimum energy paths may be analytically calculated with dislocation mechanics models **[25]**.

The reduction of layer thickness decreases point-defect concentrations and fluxes to the interface. Nevertheless, point-defect concentrations are very sensitive to sink efficiency **[26]**. Indeed, different atomic configurations results in different misfit dislocation structures that interact in turn differently with point

defects. Different void denuded zones (VDZ) widths were seen near Cu/Nb interfaces depending on their crystallographic character **[18]**. Sink efficiency of Cu/Nb_{spd} interfaces is higher than Cu/Nb_{pvd} one but none of them get decorated with voids unlike grain boundaries in nanocrystalline Cu **[27]**. Thus, synthesizing multilayer composites that remain free of voids is possible if layer thickness is reduced until VDZs near neighboring interfaces overlap.

He-irradiated Cu/Nb NMMCs are thermally stable in contrast with grains in nanocrystalline Cu that significantly coarsen **[28]**. Nevertheless, while He ions only transfer a small fraction of their kinetic energy to Cu and Nb atoms, morphological stability of Cu/Nb NMMCs may be compromised if they are irradiated with energetic neutrons or heavy ions **[29]**. Neutrons or heavy ions collide with Cu and Nb atoms initiating a ballistic phase followed by the formation of a thermal spike. The temperature reached is much higher than the melting one so a transient liquid phase forms until the energy is dissipated to surrounding atoms. Thermal spikes lead to the formation of point-defect clusters and, due to mixing across heterophase interfaces, an interfacial amorphous layer whose thickness is proportional to the square root of dose. Radiation-induced mixing is independent of interface crystallography and may be reduce by choosing low solubility metals with minimal liquid interdiffusivity as multilayer composite constituents **[30,31]**. In addition, the interdiffusion region of one interface should not overlap with the interdiffusion region of an adjacent interface to avoid layer pinchoff and, therefore, minimum layer thickness of Cu/Nb NMMCs should be between 2 and 4 nm **[29]**.

The mechanisms underlying point-defect annihilation at NMMC interfaces has been covered in enough detail at atomistic scale. Nevertheless, they are subject to time-scale limitations so a continuum approach that describes long-term evolution of point-defects in irradiated NMMCs is highly desirable. In order to provide a contribution along this line, Fadda et al. validated a mathematical model to study the dynamic behavior of vacancies and interstitials in nanostructured metallic monolayers of Cu and Nb **[32]**. Layer boundaries were described as continuum spatial distribution of sinks either neutral or variable-biased **[33]**. The effect of variation in layer thickness, temperature, point-defects production rate, and surface recombination coefficient on annihilation processes at interfaces was also addressed. In our previous work **[34]**, above model was modified to take into account interface characteristics deriving from coupling different metals and, to allow metal layers influence each other's behavior through the evolution of interfacial variable-bias sink occupation.

The present work goes a step further and compares, quantitatively, model predictions with experimental results in Cu/Nb and Cu/V NMMCs **[35]**. In such experiments, both multilayer composites were synthesized by PVD. Hence, we have focused on $\alpha/\beta\text{-}KS_{min}$ and $\text{-}KS_1$ interfaces (α = Cu and β = Nb or V). These interfaces correspond to ground-state and defect-free KS structures respectively. The former contains constitutional vacancies, whose concentration is higher in Cu/Nb interface than in Cu/V one, and, according to Mao et al., they seem to play a key role in Cu vacancy concentration dissimilarities between the two systems at the steady state. They believe that interface constitutional vacancies trap interstitials and

facilitate vacancy recombination. Moreover, the unconventional behavior of point defects in above interfaces has to be considered. Accordingly, boundary equations and initial conditions have been adapted **[34]**. Point-defect interactions with damaged and pristine boundaries tend to be different **[36]**. KS_1 may be seen as KS_{min} loaded with SIAs **[37]**. Thus, we have investigated the effect of interface SIA loading **[23]** and constitutional vacancies **[38]** on the long-term point-defect evolution. Cu/Nb- and Cu/V-KS_{min} interfaces have the same number of constitutional vacancies per MDI, however, the areal MDI density is different. Therefore, the effect of trap concentration has been analyzed too.

2. Mathematical model

We consider the same system described in our previous work **[34]**, where a layer of metal α is in between two layers of metal β (cf. **Figure 1a**). Therefore, some points explained in detail in such work will not be commented again and the reader should refer to above-mentioned reference. However, all the necessary equations that allow the model resolution will be presented here for the sake of clarity. The evolution of point defects, i.e., self-interstitial atoms (SIA) (i) and vacancies (v) concentration in layers α and β is described by the following one-dimensional spatial reaction-diffusion equations:

$$\frac{\partial C_j^{(\gamma)}}{\partial t} - D_j^{(\gamma)} \frac{\partial^2 C_j^{(\gamma)}}{\partial x^2} = K_0^{(\gamma)} - R_C^{(\gamma)} \quad j = i, v; \quad \gamma = \alpha, \beta; \tag{1}$$

along with their initial conditions

$$t = 0; \forall x \quad C_j^{(\gamma)} = {}^{*}C_j^{(\gamma)} \quad j = i, v; \quad \gamma = \alpha, \beta. \tag{2}$$

$C_j^{(\gamma)}$ is the concentration of the point defect of type *j* in layer γ, $D_j^{(\gamma)}$ is the diffusion coefficient of the point defect of type *j* in layer γ **[26]**, while $K_0^{(\gamma)}$ and $R_C^{(\gamma)}$ are the production and the recombination rates of point defects per unit volume in layer γ, respectively. ${}^{*}C_j^{(\gamma)}$ is the concentration of the point defect of type j in layer γ at thermodynamic equilibrium **[33]**. As the production rate of point defects is assumed time- and spatial-independent in each layer **[34]**, the recombination rate of point defects is expressed as a second order reaction **[33]**:

$$R_C^{(\gamma)}(x,t) = K_{iv}^{(\gamma)} \left(C_i^{(\gamma)} - {}^{*}C_i^{(\gamma)}\right)\left(C_v^{(\gamma)} - {}^{*}C_v^{(\gamma)}\right) \quad \gamma = \alpha, \beta; \tag{3}$$

where $K_{iv}^{(\gamma)}$ is the kinetic constant.

Point defects tend to get trapped in MDI regions of NMMCs interfaces **[21,22]**. In our previous work **[34]**, interfaces between metals α and β were assumed to have a surface concentration of traps for interstitials, ${}^{tot}S_i^{(\alpha-\beta)}$, and a surface concentration of traps for vacancies, ${}^{tot}S_v^{(\alpha-\beta)}$, as in Brailsford and Bullough's original work **[39]**. This means that traps for SIAs and vacancies are treated as different physical entities, which is appropriate when point defects remain compact and well localized **[13]**. However, trapped SIAs and vacancies at interfaces of multilayer composites synthesized by PVD delocalize in a similar way and form kink-jog pairs **[4]**. Thus, only one trap typology is considered in this work which is capable of accommodate both SIAs and vacancies. Moreover, point-defect delocalization significantly increases the critical distance for Frenkel-pair recombination **[11]**. So, if a point defect jumps to an interface site close to a

trapped opposite point defect, they recombine. Therefore, boundary conditions at the interface between metals α and β may be expressed as:

$$x = \frac{L}{2}; \quad \forall t \quad D_j^{(\gamma)} \frac{\partial C_j^{(\gamma)}}{\partial x} = (1 - f_j - f_k + z\, f_k)\, K_j^{(\gamma)} \left(C_j^{(\gamma)} - {}^{*}C_j^{(\gamma)}\right) \quad j = i, v; \quad k \neq j = i, v; \quad \gamma = \alpha, \beta; \tag{4}$$

where L is the thickness of layer γ and $K_j^{(\gamma)}$ is the transfer velocity of the point defect of type *j* from layer γ to the interface. A point defect may go into an unoccupied trap site, either by a SIA or a vacancy, or recombine with the nearest trapped opposite point defect, jumping there from z possible adjacent sites in the matrix. In our previous work **[34]**, z was set equal to 4 for any material structure according to Brailsford and Bullough's work. Thus, the two interface annihilation mechanisms consisting of a point defect jumping to an unoccupied trap and to an occupied trap by the opposite point defect can be considered to have a prefactor of 1 and 4 respectively. As point defects do not remain compact in PVD multilayer composites interfaces, the original physical meaning of giving z a value of 4 may be lost. Nonetheless, the effect of z value in point-defect annihilation at the interface between metals α and β has been evaluated in next section.

Point-defect trap occupation probability is obtained by solving the following balance equations:

$$\begin{aligned} \frac{df_j}{dt} = {} & (1 - f_j - f_k) \frac{K_j^{(\alpha)}}{{}^{tot}S^{(\alpha-\beta)}} \left(C_j^{(\alpha)} - {}^{*}C_j^{(\alpha)}\right) - z\, f_j \frac{K_k^{(\alpha)}}{{}^{tot}S^{(\alpha-\beta)}} \left(C_k^{(\alpha)} - {}^{*}C_k^{(\alpha)}\right) \\ & + (1 - f_j - f_k) \frac{K_j^{(\beta)}}{{}^{tot}S^{(\alpha-\beta)}} \left(C_j^{(\beta)} - {}^{*}C_j^{(\beta)}\right) - z\, f_j \frac{K_k^{(\beta)}}{{}^{tot}S^{(\alpha-\beta)}} \left(C_k^{(\beta)} - {}^{*}C_k^{(\beta)}\right) \quad j = i, v; \quad k \neq j = i, v; \\ & - \frac{\alpha_s}{{}^{tot}S^{(\alpha-\beta)}} f_j\, f_k \end{aligned} \tag{5}$$

along with their initial condition

$$t = 0, \quad f_j = f_j^0 \quad j = i, v; \tag{6}$$

where ${}^{tot}S^{(\alpha-\beta)}$ is the surface concentration of traps for point defects and α_s is the surface recombination coefficient. Temporal evolution of trap occupation probability by the point defect of type *j* depends on the fluxes of SIAs and vacancies to the interface arriving from both metal layers, α and β, and the recombination of trapped SIAs with trapped vacancies. Fadda et al. **[32]** demonstrated that point-defect evolution in a metal monolayer did not depend on α_s value. Hence, α_s has been set equal to 0 in the same way that in our previous work **[34]** where we also studied metallic multilayer composites as here. The present work focuses on KS_{min} and KS_1 interfaces **[4]**. While the latter does not possess constitutional vacancies, the former has 2-

3 vacancies per MDI **[38]**. Neither KS_{min} nor KS_1 possesses constitutional SIAs. For a temperature similar to the one of this work, it was seen that a cluster of 5-6 SIAs or vacancies added to KS_1, i.e., defect-free interface, dissociated into smaller clusters and occupied different MDIs **[24]**. Moreover, according to above study too, if a SIA or vacancy cluster is added to KS_{min}, i.e., the ground state structure, the SIAs or vacancies constituting the cluster are likely to evaporate from it and remain isolated thereafter. Therefore, it is assumed that each MDI is capable of accommodate 2-3 SIAs or vacancies. KS_{min} and KS_1 differ in the initial conditions of point-defect trap occupation probabilities, f_j^0, which may be in the range [0,1]. f_i^0 takes a nil value for both interface structures. However, f_v^0 takes a nil value for KS_1 and a unity value for KS_{min}.

By referring to **Figure 1b**, boundary conditions can be completed by the following ones. In the case of the symmetric surface of the entire system, boundary conditions may be expressed as:

$$x = 0; \quad \forall t \quad \frac{\partial C_j^{(\alpha)}}{\partial x} = 0 \quad j = i, v; \tag{7}$$

while in the case of the free surface on layer β, boundary conditions may be expressed as:

$$x = \frac{3L}{2}; \quad \forall t \quad \frac{\partial C_j^{(\beta)}}{\partial x} = 0 \quad j = i, v. \tag{8}$$

The model consisting of the balance Eqs. (1) along with their initial conditions, Eqs. (2), and their boundary conditions, i.e., Eqs. (4) in the case of the interface between metals α and β modelled as variable-biased sinks, Eqs. (7) in the case of the symmetric surface of the entire system, or Eqs. (8) in the case of the free surface, allows one to describe the spatial-temporal evolution of point-defect concentrations inside layers α and β undergoing radiation.

In order to obtain dimensionless and normalized equations and parameters, a change of variables has been used in this work following the same procedure reported previously **[34]**. Dimensionless variables and parameters, as well as scaling and reference values can be found in above work. According to this change of variables, the evolution of dimensionless point-defect concentrations in layer γ as a function of the dimensionless time is described by the following equations:

$$\frac{\partial \chi_j^{(\gamma)}}{\partial \tau} - \delta_j^{(\gamma)} \frac{\partial^2 \chi_j^{(\gamma)}}{\partial \xi^2} = A^{(\gamma)} (1 - \chi_i^{(\gamma)} \chi_v^{(\gamma)}) \qquad j = i, v; \quad \gamma = \alpha, \beta; \tag{9}$$

along with the initial conditions

$$\tau = 0; \forall \xi \quad \chi_j^{(\gamma)} = 0 \qquad j = i, v; \quad \gamma = \alpha, \beta; \tag{10}$$

At the interface between metals α and β modelled as variable biased sinks, dimensionless boundary conditions may be expressed as:

$$\xi = \frac{1}{3}; \forall \tau \quad \delta_j^{(\gamma)} \frac{\partial \chi_j^{(\gamma)}}{\partial \xi} = \frac{3}{2}(1 - f_j - f_k + z\, f_k) \frac{\delta_j^{(\gamma)}}{\varpi^{(\gamma)}} \chi_j^{(\gamma)} \quad j = i, v; \quad k \neq j = i, v; \quad \gamma = \alpha, \beta; \tag{11}$$

The dimensionless balance equations of trap occupation probabilities appear as follows:

$$\begin{aligned} \frac{df_j}{d\tau} = {} & E_j^{(\alpha)} \left[(1 - f_j - f_k) \frac{\delta_j^{(\alpha)}}{\varpi^{(\alpha)}} \chi_j^{(\alpha)} - z\, f_j \frac{\delta_k^{(\alpha)}}{\varpi^{(\alpha)}} \chi_k^{(\alpha)} \right] \\ & + E_j^{(\beta)} \left[(1 - f_j - f_k) \frac{\delta_j^{(\beta)}}{\varpi^{(\beta)}} \chi_j^{(\beta)} - z\, f_j \frac{\delta_k^{(\beta)}}{\varpi^{(\beta)}} \chi_k^{(\beta)} \right] \quad j = i, v; \quad k \neq j = i, v; \\ & - F_j f_j f_k \end{aligned} \tag{12}$$

along with their initial conditions

$$\tau = 0, \quad f_j = f_j^0 \quad j = i, v; \tag{13}$$

Dimensionless boundary conditions for the symmetric surface of the entire system may be expressed as:

$$\xi = 0; \quad \forall \tau \quad \frac{\partial \chi_j^{(\alpha)}}{\partial \xi} = 0 \quad j = i, v; \tag{14}$$

while dimensionless boundary conditions representing the free surface on layer β as:

$$\xi = 1; \quad \forall \tau \quad \frac{\partial \chi_j^{(\beta)}}{\partial \xi} = 0 \quad j = i, v; \tag{15}$$

Average dimensionless concentration and net-production rate of the point defect of type j in layer γ, $\overline{\chi}_j^{(\gamma)}$ and $\overline{\Pi}^{(\gamma)}$ respectively, as well as dimensionless flux of the point defect of type j from layer γ to the interface between metals α and β, $J_j^{(\gamma)}$, have been defined as in our previous work **[34]** with the aim of illustrating and discussing model results. Model equations are solved by using the commercial software

COMSOL Multiphysics 3.4, along with the parameters for Cu, Nb and V reported in our previous work **[34]** except the value of parameter z, which has been evaluated in next section before setting it, and ${}^{tot}S^{(\alpha-\beta)}$, which have been set equal to 2.5 times the values of ${}^{tot}S_j^{(\alpha-\beta)}$ reported in above work. The latter is due to KS_{min} and KS_1 capacity to accommodate 2-3 SIAs or vacancies in each MDI as it has been explained previously.

3. Results

In what follows, copper is represented by metal α while metal β is niobium, or vanadium. Results are shown in a double-log plot (**Figures 2-9**) and they are obtained by solving the dimensionless version of the model illustrated in the previous section. All the results belong to the half-symmetric part of the layered system depicted in **Figure 1**. Firstly, the effect of parameter z value in point-defect evolution is evaluated as it has been indicated previously. This parametric sensitivity is performed in Cu/Nb NMMCs for either KS_{min} or KS_1 interface configuration. Three z values are considered, 0, 1 and 4. It should be noted that a nil value of parameter z for KS_1 permits point defects in the matrix to jump only to unoccupied traps, canceling the mechanism consisting in the recombination of a point defect jumping from the matrix with the nearest trapped opposite point defect (cf. Eq. (4)). For KS_{min}, a nil value of parameter z cancels both interface annihilation mechanisms and suppresses point-defect fluxes. This last case represents the absence of point-defect traps.

The corresponding temporal profiles of average point-defect concentrations in Cu and Nb layers of Cu/Nb system for the different values of z are shown in **Figures 2** and **3**, respectively. It can be seen in **Figure 2a** that $\bar{\chi}_i^{(\alpha)}$ constantly increases from the equilibrium concentration until $\tau \approx 0.2$. This behavior can be observed for all z values and for both interface configurations except for KS_{min} with z =0. In this case, $\bar{\chi}_i^{(\alpha)}$ continues increasing until $\tau \approx 10^3$. Then, average concentration of SIAs remains constant up to $\tau \approx 10^7$ in Cu layer. However, there is a different evolution for KS_1 with z =0. Indeed, $\bar{\chi}_i^{(\alpha)}$ abruptly increases to reach a stationary SIA average concentration. **Figure 2b** shows the temporal evolution of vacancy average concentration in Cu layer. Initially, $\bar{\chi}_v^{(\alpha)}$ increases until longer times than $\bar{\chi}_i^{(\alpha)}$ except for KS_{min} with z =0. In this case, vacancy and SIA average concentration in Cu layer show the same behavior. Similarly to $\bar{\chi}_i^{(\alpha)}$, no differences can be observed for KS_1 between the three values of z until $\tau \approx 10^7$. Then, $\bar{\chi}_v^{(\alpha)}$ also increases abruptly for z =0 to reach a stationary vacancy average concentration. In contrast, $\bar{\chi}_v^{(\alpha)}$ achieves a maximum for KS_{min} with z equal to 1 and 4, to then decrease until steady state is reached. In all cases, the stationary value of $\bar{\chi}_v^{(\alpha)}$ is higher compared to the stationary value of $\bar{\chi}_i^{(\alpha)}$ except for KS_{min} with z =0 that is equal.

Figures 3a and **3b** show the temporal profiles of SIA and vacancy average concentrations in Nb layer respectively for the different values of z. It can be seen a similar behavior of $\bar{\chi}_i^{(\beta)}$ compared to $\bar{\chi}_i^{(\alpha)}$ for both interface configurations with the different values of z. The same occurs with $\bar{\chi}_v^{(\beta)}$ with respect to $\bar{\chi}_v^{(\alpha)}$, although, some differences can be observed either in SIA or vacancy average concentrations. Firstly, $\bar{\chi}_i^{(\beta)}$ decreases between $\tau \approx 10^5$ and $\tau \approx 10^7$ for all the cases studied except for KS_{min} with z =0. Secondly, $\bar{\chi}_v^{(\beta)}$ does not reach a maximum and decreases before steady state as $\bar{\chi}_v^{(\alpha)}$ for KS_{min} with z equal to 1 and 4. Instead, a stationary vacancy average concentration is reached in Nb layer after the initial increase. So, according to the results of **Figures 2** and **3** for the different values of parameter z, the overweighting of the mechanism consisting in the recombination of a point defect jumping from the matrix with the nearest

trapped opposite point defect seems not to be effective. Indeed, point-defect evolution is not affected by the increase of z value from 1 to 4 either for KS_{min} or KS_1. Therefore, the value of parameter z is set equal to 1 and the following results correspond to this value. The effect of no interface recombination (KS_1 with z =0) and point-defect traps absence (KS_{min} with z =0) is analyzed more extensively in the discussion section.

Now, a comparison between the respond of Cu/Nb and Cu/V systems to irradiation for KS_{min} and KS_1 interface configuration is performed. Some details commented previously for Cu/Nb system would not be analyzed again and the reader should refer to above paragraphs. The corresponding temporal profiles of average point-defect concentrations in layers α (Cu) and β (Nb, or V) are depicted in **Figures 4** and **5**, respectively. It can be seen in **Figure 4a** that $\bar{\chi}_i^{(\alpha)}$ does not show any difference between Cu/Nb and Cu/V systems and neither does it between KS_{min} and KS_1. Similarly, $\bar{\chi}_v^{(\alpha)}$ exhibits the same behavior for KS_1 in both systems (**Figure 4b**). On the contrary, there is a different evolution of $\bar{\chi}_v^{(\alpha)}$ depending on the interface configuration for each system, Cu/Nb or Cu/V. This can be seen too when comparing Cu/Nb to Cu/V for KS_{min}.

Figures 5a and **5b** show the temporal profiles of SIA and vacancy average concentrations in layer β respectively. In contrast to $\bar{\chi}_i^{(\beta)}$ in Cu/Nb system that decreases before reaching steady state, SIA average concentration in V layer maintains the stationary value reached after the initial increase during the rest of irradiation time. Furthermore, there are no differences in the evolution of $\bar{\chi}_i^{(\beta)}$ between KS_{min} and KS_1 in Cu/V system unlike in Cu/Nb one. Even though $\bar{\chi}_v^{(\beta)}$ initially increases to reach a stationary value in all the cases studied except for Cu/V-KS_{min} system, where $\bar{\chi}_v^{(\beta)}$ reaches a maximum and decreases before reaching steady state, significant dissimilarities can be observed in the temporal profiles of vacancy average concentration in layer β.

The investigation of point-defect production, transport and annihilation phenomena may help to explain differences and similarities shown in the temporal evolution of point-defect average concentrations between the systems studied. Point-defect production rates in layers α and β are constant temporally and spatially but, they have a different value for each metal **[34]**. On the contrary, point-defect recombination rates in layers α and β depend upon SIA and vacancy concentrations in layer α and β respectively. Thus, the corresponding temporal profiles of the average point-defect net-production rate in layers α and β, which are the result of combining point-defect production phenomena with recombination one, are shown in **Figures 6a** and **6b**, respectively. It can be seen in **Figure 6a** that $\bar{\Pi}^{(\alpha)}$ keeps constant at any time for both systems investigated, Cu/Nb and Cu/V, and both interface configuration considered, KS_{min} and KS_1. This can be considered to occur too in $\bar{\Pi}^{(\beta)}$ (**Figure 6b**) for Cu/V system as the decrease observed for KS_{min} is very small. On the other hand, average point-defect net-production rate in Nb layer shows a significant decrease, which is more notable for KS_{min} than for KS_1, before steady-state is reached.

Point-defect flux to the interface between the two metals represents the other mechanism affecting point-defect annihilation in addition to bulk recombination. The corresponding temporal profiles of point-

defect fluxes from layer α and layer β to the interface between the two metals are reported in **Figures 7** and **8**, respectively. It can be seen in **Figure 7a** that $J_i^{(\alpha)}$ shows the same behavior for all the systems investigated. The higher diffusivity of SIAs allows them to get the interface between metals faster than vacancies. Consequently, SIA flux achieves a maximum earlier than vacancy one (cf. **Figures 7a** and 7**b**). There are no differences in the evolution of $J_v^{(\alpha)}$ between both systems, Cu/Nb and Cu/V, but only for KS_1, not for KS_{min}.

It can be seen in **Figure 8a** that $J_i^{(\beta)}$ increases to reach a stationary value for all the cases considered. Only SIA flux from layer β in Cu/V-KS_1 system maintains this value during the whole irradiation exposure. For the rest of cases, $J_i^{(\beta)}$ decreases before reaching steady state. The significance of the decrease is very small in Cu/V system for KS_{min}. In Cu/Nb system, the decrease is more notable for KS_{min} than for KS_1. **Figure 8b** shows that vacancy flux from layer β strongly depend upon the system investigated and the interface configuration. It should be noted that, once the steady state is reached, the fluxes of SIAs and vacancies from layer α, or layer β, to the interface have the same value for each particular system and interface configuration.

Besides the transfer velocity of point defects to the interface, which does not generate differences in layer α since it is the same metal (Cu) for all the systems investigated, point-defect flux relies on point-defect concentration at the interface and point-defect trap occupation probability (cf. Eq. (4)). Despite the differences between the values of point-defect concentration at the interface and point-defect average concentration, their temporal profiles show a very similar behavior. So, the former are not shown here. On the other hand, and lastly, temporal profiles of trap occupation probabilities by point defects are depicted in **Figure 9**. Trap occupation probability by SIAs (**Figure 9a**) increases and then it reaches a stationary state for all the cases studied. It can be also seen that the stationary value is higher for KS_1 than for KS_{min} in both systems, Cu/Nb and Cu/V. Steady state is reached sooner by Cu/V system than by Cu/Nb one either for KS_1 or KS_{min}. The stationary value of f_i is the same in both systems for KS_1 but not for KS_{min}. For this case, the steady-state value of f_i is higher for Cu/Nb system than for Cu/V one. Vacancy trap occupation probability shows a similar behavior to SIA one for KS_1 in both systems (cf. **Figure 9a** and **9b**). Nevertheless, f_v behaves very different for KS_{min} due to the initial condition.

4. Discussion

Thin layered systems are designed with the aim to increase interfaces density. The higher the available surface for annihilation of point defects, the lower their concentration within the system. This was demonstrated at very different time scales **[17,26]**. Cu/Nb interfaces synthesized by PVD are virtually inexhaustible sinks for radiation-induced point defects **[4,11]**. SIA and vacancy delocalization allows long-range interactions between them which facilitate Frenkel-pair recombination. Cu SIAs are loaded at Cu/Nb interfaces during the collision cascades and their subsequent emission promotes enhanced recombination near the interface **[23]**. However, the effect of interface point-defect trapping and recombination mechanisms on the long-term evolution of point defects has not been investigated. So, before comparing model predictions in Cu/Nb and Cu/V NMMCs, it is worth discussing the influence of above mechanisms on point-defect concentrations.

Temporal profiles of average SIA and vacancy concentrations in Cu and Nb layers of Cu/Nb system for the different values of z are shown in **Figures 2** and **3**, respectively. In previous section, it has been stated that point-defect evolution is not affected by the increase of z value from 1 to 4 either for KS_{min} or KS_1. KS_{min}, i.e., ground state structure, along a value of z equal to 1, can be considered the reference case among the cases studied as it is the one that most accurately represents reality in multilayer composites synthesized by PVD. On the other hand, KS_1, i.e., defect-free structure, can be seen as KS_{min} loaded with SIAs. Thus, interface SIA loading (KS_1 with z =1) decreases steady-state values of vacancy average concentration in Cu and Nb layers with respect to the reference case (cf. **Figures 2b** and **3b** respectively) while, on the contrary, the stationary SIA average concentration value does not show any difference in Cu layer (cf. **Figure 2a**) or increases slightly in Nb one (cf. **Figure 3a**). These value differences are caused by dissimilarities on the evolution of average point-defect net-production rate and/or point-defect flux to the interface between metals. Either in Cu or Nb layer, the higher flux of vacancies for KS_1 (cf. **Figures 7b** and **8b** respectively) results in the lower value of vacancy average concentration. On the contrary, the higher point-defect net-production rate for KS_1 (cf. **Figure 6b**) is responsible of the higher SIA average concentration value in Nb layer.

For KS_1, temporal profiles of point-defect average concentrations are independent of z value up to $\tau \approx 10^7$. But then, if point-defect trapping is allowed but point-defect recombination at the interface is not (KS_1 with z =0), point-defect average concentrations increase (cf. **Figures 2** and **3**) until bulk recombination compensates the suppression of point-defect flux to the interface due to the saturation of traps by SIAs and vacancies, i.e., $f_i + f_v = 1$ (results not shown here). So, with respect to the equivalent case in which interface recombination is allowed (KS_1 with z =1), it can be concluded that either SIA or vacancy average concentration at steady state increases when no recombination of point defects occurs at the interface. If neither point-defect trapping nor point-defect recombination at the interface are allowed (KS_{min} with z =0), steady-state value of SIA and vacancy average concentration increases and decreases respectively in comparison to the rest of cases studied (cf. **Figures 2** and **3**). This case represents the absence of traps for

point defects. Since there is no point-defect flux to the interface between metals, the only annihilation mechanism of point defects is the bulk recombination and, consequently, evolution of SIA and vacancy average concentration show the same behavior.

Now, a comparison between point-defect concentrations within the systems investigated is performed. Especial attention is paid to the behavior of the same metal Cu (layer α), when it is surrounded by diverse metals β (Nb, or V). Cu/V_{pvd} interfaces are capable of accommodate 2-3 SIAs or vacancies per MDI as Cu/Nb_{pvd} ones but their areal MDI density is different **[38]**. According to Mao et al. **[35]**, constitutional vacancies seem to play an important role in Cu vacancy concentration dissimilarities between the two systems studied at the steady state. So, numerical simulation results for KS_{min} and KS_1 interface configurations are compared too. Temporal profiles of average SIA and vacancy concentrations in layers α and β are represented in **Figures 4** and **5**, respectively. SIA average concentration in layer α show the same behavior for all the cases studied (cf. **Figure 4a**). This is due to the absence of differences in $\overline{\Pi}^{(\alpha)}$ (cf. **Figure 6a**) and $J_i^{(\alpha)}$ (cf. **Figure 7a**). On the other hand, a general comparison of the results reveals that vacancy average concentration in layer α group by interface configurations, KS_{min} or KS_1 (cf. **Figure 4b**), while in layer β, SIA and vacancy average concentration group by system, Cu/Nb or Cu/V (cf. **Figures 5a** and **5b** respectively). However, differences can be found between the cases that belong to each group except in $\bar{\chi}_v^{(\alpha)}$ for KS_1. The lower steady-state values of $\bar{\chi}_v^{(\alpha)}$ correspond to Cu/Nb- and Cu/V-KS_1 systems (cf. **Figure 4b**) and are the result of a higher $J_v^{(\alpha)}$ before reaching a stationary state (cf. **Figure 7b**). For KS_{min}, dissimilarities in $\bar{\chi}_v^{(\alpha)}$ between Cu/Nb and Cu/V systems are caused by differences in vacancy flux from layer α too. $J_v^{(\alpha)}$ reaches steady state in Cu/V system but, in Cu/Nb one, vacancy flux from layer α continues increasing for a while (cf. inset of **Figure 7b**) because f_v decrease (recalling boundary condition (11) and cf. inset of **Figure 9b**). This causes that, between $\tau \approx 3\ 10^5$ and $\tau \approx 2\ 10^6$, the vacancies annihilated at the interface are more than the vacancies produced in layer α which decreases $\bar{\chi}_v^{(\alpha)}$ in Cu/Nb system (cf. **Figure 4b**). Consequently, steady-state value of $\bar{\chi}_v^{(\alpha)}$ is lower in Cu/Nb system than in Cu/V one for KS_{min}. Before comparing vacancy-concentration results in layer α to results reported in **Ref. (35)**, point-defect concentrations in layer β are analyzed too. Differences in the steady-state value of $\bar{\chi}_i^{(\beta)}$ and $\bar{\chi}_v^{(\beta)}$ between the four cases investigated can be explained by means of the evolution of $\overline{\Pi}^{(\beta)}$ and $J_v^{(\beta)}$ respectively. Thus, the higher the average point-defect net-production rate in layer β at longer times (cf. **Figure 6b**), the higher the stationary value of SIA average concentration (cf. **Figure 5a**). And, the higher the vacancy flux from layer β to the interface at longer times (cf. **Figure 8b**), the lower the stationary value of vacancy average concentration (cf. **Figure 5b**). As in $\bar{\chi}_v^{(\alpha)}$ for Cu/Nb-KS_{min} system, there is an interval in which $\bar{\chi}_v^{(\beta)}$ decreases for Cu/V-KS_{min} system (cf. **Figures 4b** and **5b**). Mechanisms illustrated above are also responsible of this effect in this case. This confirms that the decrease of vacancy average concentration seen before reaching steady state in Cu layer of Cu/Nb system and V layer of Cu/V one for KS_{min} is due to the

lower diffusion coefficient of vacancies in the other metal, niobium and copper respectively. So, in short, the respond to irradiation of the systems investigated here depends on both, interface characteristics and bulk properties. The presence of interface constitutional vacancies makes decrease the concentration of SIAs slightly, if at all, and increase the concentration of vacancies significantly in each system.

Lastly, vacancy-concentration results in layer α are compared to results reported in **Ref. (35)**. According to experimental results, vacancy concentration at the center of 30-nm Cu layer was 1.9 times lower in Cu/Nb system than in Cu/V one. Similar predictions, a factor of 2 instead of 1.9, were obtained for vacancy average concentration in kinetic Monte Carlo simulations. As commented previously, the case that most accurately represents reality in multilayer composites synthesized by PVD corresponds to KS_{min} interface configuration along a z value equal to 1. For this case, vacancy concentration at the center of Cu layer (results not shown here due to the similitudes with vacancy average concentration) and $\bar{\chi}_v^{(\alpha)}$ (cf. **Figure 4b**) are approximately 1.8 and 1.9 times lower respectively in Cu/Nb system than in Cu/V one. Mao et al. associated the lower Cu vacancy concentration in Cu/Nb-KS_{min} system to its higher probability of absorbing a vacancy at the interface. Either Cu/Nb_{pvd} or Cu/V_{pvd} interfaces are capable of accommodate 2-3 SIAs or vacancies per MDI but the areal MDI density is ~6.4 times higher in Cu/Nb_{pvd} interface than in Cu/V_{pvd} one. However, the lower the point-defect trap concentration, the lower the vacancy average concentration according to our results (KS_{min} with z =0). So, the explanation for above factor values, ~1.8 and ~1.9, points to the diffusivity of vacancies that is lower in copper than in niobium and makes Cu vacancy concentration decrease in Cu/Nb system before reaching steady state. This results in a stationary value which is lower than in Cu/V system. In spite of the very good qualitative agreement between experimental results and our model predictions, it is worth to discuss some details. The production rate of Frenkel pairs has been calculated for copper, niobium, and vanadium layers with the irradiation conditions reported in **Ref. (35)** using Transport of Ions in Matter (TRIM) **[40]**. Then, a factor of 10^{-2} has been applied. According to Mao et al., this normalization achieved a perfect agreement between the absolute concentrations of Cu vacancies calculated in their rate-theory model and the experimental data. Nevertheless, a factor of ~2.41 10^{-4} and ~1.17 10^{-4} is needed in Cu/Nb and Cu/V system respectively with our model which is quite smaller than 10^{-2}. Experimental results are given only in Cu layer (layer α) so it would be recommendable to have vacancy concentration in layer β (Nb, or V) too. Thus, it could be estimated a factor for each metal layer.

5. Conclusions

A continuum model of point-defect evolution in multilayer composites is presented in this work. In order to compare quantitatively model predictions with experimental results in multilayer composites synthesized by PVD **[35]**, previous work boundary equations and initial conditions **[34]** have had to be adapted. Firstly, the effect of interface annihilation mechanisms on the long-term evolution of point defects has been studied. If SIAs and vacancies can be trapped but cannot recombine with the opposite point defect at the interface between metals, SIA and vacancy concentrations within the system increase. However, if none of the two mechanisms is operative, i.e., absence of traps for point defects, SIAs and vacancies behave similarly which leads to a rise and a drop in the concentration of SIAs and vacancies respectively. In addition, the effect of interface SIA loading and constitutional vacancies has been investigated too by comparing the results corresponding to KS_{min} and KS_1 interface configuration. The presence of interface constitutional vacancies makes decrease the concentration of SIAs slightly, if at all, and increase the concentration of vacancies significantly. The latter is in agreement with VDZ measurements **[18]** that reveal a higher sink efficiency in Cu/Nb_{spd} interfaces **[13]** than in Cu/Nb_{pvd} ones **[4]** for vacancies. On the contrary, interface SIA loading has the reverse effect to the presence of constitutional vacancies at the interface. The emission of SIAs loaded at the interface promotes enhanced recombination near the interface according to Liu et al. **[23]**. So, this agrees too with our results that predict a significant decrease of vacancy concentration when SIAs are loaded at the interface.

The respond to irradiation of the systems investigated here, Cu/Nb and Cu/V, depends on both, interface characteristics and bulk properties. It is worth highlighting that point-defect flux to the interface depends upon the value of point-defect trap concentration, which is characteristic of each metal couple α-β, and the properties of the two adjacent layers (recalling boundary condition (4)). However, the influence of the properties of one metal in the point-defect evolution of the other metal is only effective if there are constitutional vacancies at the interface, i.e., for KS_{min}. This can be seen in the temporal evolution of vacancies. The concentration of vacancies decreases before reaching steady state in Cu layer of Cu/Nb system because the diffusivity of vacancies is lower in niobium than in copper. It occurs similarly in V layer of Cu/V system. A comparison of model results for KS_{min} shows no differences between Cu/Nb and Cu/V system regarding SIA temporal evolution in copper (layer α), while in layer β, SIA concentration at steady state is lower in niobium than in vanadium. On the other hand, the lower steady-state value of vacancy concentration in layer α and β correspond to Cu/Nb and Cu/V system respectively for KS_{min}. Irradiated Cu/Nb NMMCs had numerous voids in Cu layers at the end of the experiment but no voids were seen in Nb layers due to the high and low mobility of vacancies respectively in these metal layers **[18]**. Hence, the high concentration of vacancies in Nb layer should not be an issue in terms of damage.

As a final conclusion, there is a very good qualitative agreement between our model predictions and results reported in **Ref. (35)**. Indeed, vacancy concentration at the center of Cu layer and average one are approximately 1.8 and 1.9 times lower respectively in Cu/Nb system than in Cu/V one for KS_{min}. So that the

agreement is quantitative too, a factor of ~2.41 10^{-4} and ~1.17 10^{-4} should be applied in Cu/Nb and Cu/V system respectively to the production rate of Frenkel pairs calculated using TRIM for each layer (Cu, Nb, or V) instead the factor of 10^{-2} suggested by Mao et al. and used in the present work. The small value of above factors could mean that, although Cu vacancy concentration differences between Cu/Nb- and Cu/V-KS_{min} systems are determined at longer time scales, multilayer composites designed at the nanometric scale may be governed by mechanisms that occurs in lower time scales. In the case of having also experimental vacancy concentration in layer β (Nb, or V) too and not only in Cu (layer α), it could be estimated a factor for each metal layer that in turn may allow relating interface characteristics and bulk properties with the magnitude of the factor. After validation with data of experiments carried out in other systems, point-defect concentrations may be calculated for any NMMC whose properties were known without the need of further experiments or atomistic simulations.

Nomenclature

A dimensionless production rate of point defects, -;

C concentration of point defects, m^{-3};

D diffusivity, $m^2\ s^{-1}$;

E dimensionless parameter of point-defect jumps from the matrix, -;

F dimensionless parameter of point-defect surface recombination, -;

f trap occupation probability, -;

K transfer velocity, $m\ s^{-1}$;

K_{iv} recombination factor of the anti-defects, $m^3\ s^{-1}$;

K_0 production rate of point defects, $m^{-3}\ s^{-1}$;

L layer thickness, m;

R_C removal rate of point defects due to recombination, $m^{-3}\ s^{-1}$;

${}^{tot}S$ concentration of traps for point defects, m^{-2};

t time, s;

x spatial coordinate, m;

z number of jumps, -;

Greek letters

α_s surface recombination coefficient, $m^{-2}\ s^{-1}$;

χ dimensionless concentration of point defects, -;

δ dimensionless diffusivity, -;

τ dimensionless time, -;

ϖ dimensionless lattice spacing, -;

ξ dimensionless spatial coordinate, -;

Superscripts

* equilibrium;

$^{(\alpha)}$ layer of element α;

$^{(\gamma)}$ layer of element γ;

$^{(\beta)}$ layer of element β;

$^{(\alpha\text{-}\beta)}$ system formed by elements α and β;

Subscripts

$_i$ self-interstitial atom;

$_j$ point defect of the type j;

$_v$ vacancy.

Acknowledgments

This work has been supported by the European Social Fund, Operational Programme of Castilla y León, and Junta de Castilla y León, through the Ministry of Education, as well as by the European Union Framework Programme 7, Multiscale Modelling and Materials by Design of Interface-Controlled Radiation Damage in Crystalline Materials (RADINTERFACES) under grant agreement no. 263273.

Conflicts of Interest

The authors declare that the supports do not lead to any conflict of interest. The authors also declare that there are no possible conflicts of interest related to this manuscript.

References

[1] A. Misra, M. J. Demkowicz, X. Zhang, and R. G. Hoagland, "The radiation damage tolerance of ultra-high strength nanolayered composites", *JOM: Journal of the Minerals, Metals and Materials Society*, vol. 59, no. 9, pp. 62-65, 2007.

[2] M. J. Demkowicz, P. Bellon, and B. D. Wirth, "Atomic-scale design of radiation-tolerant nanocomposites", *MRS bulletin*, vol. 35, no. 12, pp. 992-998, 2010.

[3] D. L. Medlin, M. J. Demkowicz, and E. A. Marquis, "Solid State interfaces: Toward an atomistic-scale understanding of structure, properties, and behavior", *JOM: Journal of the Minerals, Metals and Materials Society*, vol. 62, no. 12, pp. 52-52, 2010.

[4] M. J. Demkowicz, J. I. A. N. Wang, and R. G. Hoagland, "Interfaces between dissimilar crystalline solids", *Dislocations in solids*, vol. 14, pp. 141-207, 2008.

[5] G. Kurdjumow and G. Sachs, "Über den mechanismus der stahlhärtung", *Zeitschrift für Physik*, vol. 64, no. 5-6, pp. 325-343, 1930.

[6] Z. Nishiyama, "X-ray investigation of the mechanism of the transformation from face centered cubic lattice to body centered cubic", *Science Reports of the Tohoku Imperial University*, vol. 23, pp. 637-664, 1934.

[7] G. Wassermann, "Üeber den Mechanismus der α-γ-Umwandlung des Eisens", Mitteilungen aus dem Kaiser Wilhelm-Institut für Eisenforschung zu Düsseldorf, Verlag Stahleisen, 1935.

[8] M. J. Demkowicz and R. G. Hoagland, "Structure of Kurdjumov–Sachs interfaces in simulations of a copper–niobium bilayer", *Journal of Nuclear Materials*, vol. 372, no. 1, pp. 45-52, 2008.

[9] A. J. Vattré and M. J. Demkowicz, "Determining the Burgers vectors and elastic strain energies of interface dislocation arrays using anisotropic elasticity theory", *Acta Materialia*, vol. 61, no. 14, pp. 5172-5187, 2013.

[10] A. J. Vattré and M. J. Demkowicz, "Partitioning of elastic distortions at a semicoherent heterophase interface between anisotropic crystals", *Acta Materialia*, vol. 82, pp. 234-243, 2015.

[11] M. J. Demkowicz, R. G. Hoagland, and J. P. Hirth, "Interface structure and radiation damage resistance in Cu-Nb multilayer nanocomposites", *Physical review letters*, vol. 100, no. 13, article 136102, 2008.

[12] S. A. Skirlo and M. J. Demkowicz, "Viscoelasticity of stepped interfaces", *Applied Physics Letters*, vol. 103, no. 17, article 171908, 2013.

[13] M. J. Demkowicz and L. Thilly, "Structure, shear resistance and interaction with point defects of interfaces in Cu–Nb nanocomposites synthesized by severe plastic deformation", *Acta materialia*, vol. 59, no. 20, pp. 7744-7756, 2011.

[14] J. Wang, R. G. Hoagland, X. Y. Liu, and A. Misra, "The influence of interface shear strength on the glide dislocation–interface interactions", *Acta Materialia*, vol. 59, no. 8, pp. 3164-3173, 2011.

[15] A. A. Sagüés and J. Auer, "Mechanical behavior of Nb-1% Zr implanted with He at various temperatures", no. CONF-750989-P2, 1976.

[16] N. Li, M. J. Demkowicz, and N. A. Mara, "Microstructure Evolution and Mechanical Response of Nanolaminate Composites Irradiated with Helium at Elevated Temperatures", *JOM: Journal of the Minerals, Metals and Materials Society*, vol. 69, no. 11, pp. 2206-2213, 2017.

[17] M. J. Demkowicz and R. G. Hoagland, "Simulations of collision cascades in Cu–Nb layered composites using an eam interatomic potential", *International Journal of Applied Mechanics*, vol. 1, no. 3, pp. 421-442, 2009.

[18] W. Han, M. J. Demkowicz, N. A. Mara, E. Fu, S. Sinha, A. D. Rollett, Y. Wang, J. S. Carpenter, I. J. Beyerlein, and A. Misra, "Design of radiation tolerant materials via interface engineering", *Advanced materials*, vol. 25, no. 48, pp. 6975-6979, 2013.

[19] C. González, R. Iglesias, and M. J. Demkowicz, "Point defect stability in a semicoherent metallic interface", *Physical Review B*, vol. 91, no. 6, article 064103, 2015.

[20] S. L. Dudarev, "Density functional theory models for radiation damage", *Annual Review of Materials Research*, vol. 43, pp. 35-61, 2013.

[21] X. Y. Liu, R. G. Hoagland, J. Wang, T. C. Germann, and A. Misra, "The influence of dilute heats of mixing on the atomic structures, defect energetics and mechanical properties of fcc–bcc interfaces", *Acta Materialia*, vol. 58, no. 13, pp. 4549-4557, 2010.

[22] X. Y. Liu, R. G. Hoagland, M. J. Demkowicz, Michael Nastasi, and A. Misra, "The influence of lattice misfit on the atomic structures and defect energetics of face centered cubic–body centered cubic interfaces", *Journal of Engineering Materials and Technology*, vol. 134, no. 2, article 021012, 2012.

[23] X. Y. Liu, B. P. Uberuaga, M. J. Demkowicz, T. C. Germann, A. Misra, and M. Nastasi, "Mechanism for recombination of radiation-induced point defects at interphase boundaries", *Physical Review B*, vol. 85, no. 1, article 012103, 2012.

[24] K. Kolluri and M. J. Demkowicz, "Formation, migration, and clustering of delocalized vacancies and interstitials at a solid-state semicoherent interface", *Physical Review B*, vol. 85, no. 20, article 205416, 2012.

[25] K. Kolluri and M. J. Demkowicz, "Dislocation mechanism of interface point defect migration", *Physical Review B*, vol. 82, no. 19, article 193404, 2010.

[26] M. J. Demkowicz, R. G. Hoagland, B. P. Uberuaga, and A. Misra, "Influence of interface sink strength on the reduction of radiation-induced defect concentrations and fluxes in materials with large interface area per unit volume", *Physical Review B*, vol. 84, no. 10, article 104102, 2011.

[27] W. Z. Han, M. J. Demkowicz, E. G. Fu, Y. Q. Wang, and A. Misra, "Effect of grain boundary character on sink efficiency", *Acta materialia*, vol. 60, no. 18, pp. 6341-6351, 2012.

[28] W. Han, E. G. Fu, M. J. Demkowicz, Y. Wang, and A. Misra, "Irradiation damage of single crystal, coarse-grained, and nanograined copper under helium bombardment at 450 C", *Journal of Materials Research*, vol. 28, no. 20, pp. 2763-2770, 2013.

[29] L. Zhang and M. J. Demkowicz, "Morphological stability of Cu-Nb nanocomposites under high-energy collision cascades", *Applied Physics Letters*, vol. 103, no. 6, article 061604, 2013.

[30] L. Zhang, E. Martinez, A. Caro, X. Y. Liu, and M. J. Demkowicz, "Liquid-phase thermodynamics and structures in the Cu–Nb binary system", *Modelling and Simulation in Materials Science and Engineering*, vol. 21, no. 2, article 025005, 2013.

[31] L. Zhang and M. J. Demkowicz, "Radiation-induced mixing between metals of low solid solubility", *Acta Materialia*, vol. 76, pp. 135-150, 2014.

[32] S. Fadda, A. M. Locci, and F. Delogu, "Modeling of point defects annihilation in multilayered Cu/Nb composites under irradiation", *Advances in Materials Science and Engineering*, vol. 2016, Article ID 9435431, 17 pages, 2016.

[33] G. S. Was, *Fundamentals of radiation materials science – Metals and alloys*, Springer, 2007.

[34] J. Ortún-Palacios, A. M. Locci, S. Fadda, F. Delogu, and S. Cuesta-López, "Role of interface in multilayered composites under irradiation: a mathematical investigation", *Advances in Materials Science and Engineering*, vol. 2017, Article ID 1079735, 16 pages, 2017.

[35] S. Mao, S. Shu, J. Zhou, R. S. Averback, and S. J. Dillon, "Quantitative comparison of sink efficiency of Cu-Nb, Cu-V and Cu-Ni interfaces for point defects", *Acta Materialia*, vol. 82, pp. 328-335, 2015.

[36] I. J. Beyerlein, A. Caro, M. J. Demkowicz, N. A. Mara, A. Misra, and B. P. Uberuaga, "Radiation damage tolerant nanomaterials", *Materials today*, vol. 16, no. 11, pp. 443-449, 2013.

[37] M. G. McPhie, L. Capolungo, A. Y. Dunn, and M. Cherkaoui, "Interfacial trapping mechanism of He in Cu–Nb multilayer materials", *Journal of Nuclear Materials*, vol. 437, no. 1-3, pp. 222-228, 2013.

[38] M. J. Demkowicz, A. Misra, and A. Caro, "The role of interface structure in controlling high helium concentrations", *Current opinion in solid state and materials science*, vol. 16, no. 3, pp. 101-108, 2012.

[39] A. D. Brailsford and R. Bullough, "The rate theory of swelling due to void growth in irradiated metals", *Journal of Nuclear Materials*, vol. 44, no. 2, pp. 121-135, 1972.

[40] J. F. Ziegler, *Transport of Ions in Matter* (TRIM), IBM Corp. Software, 1991.

Figures

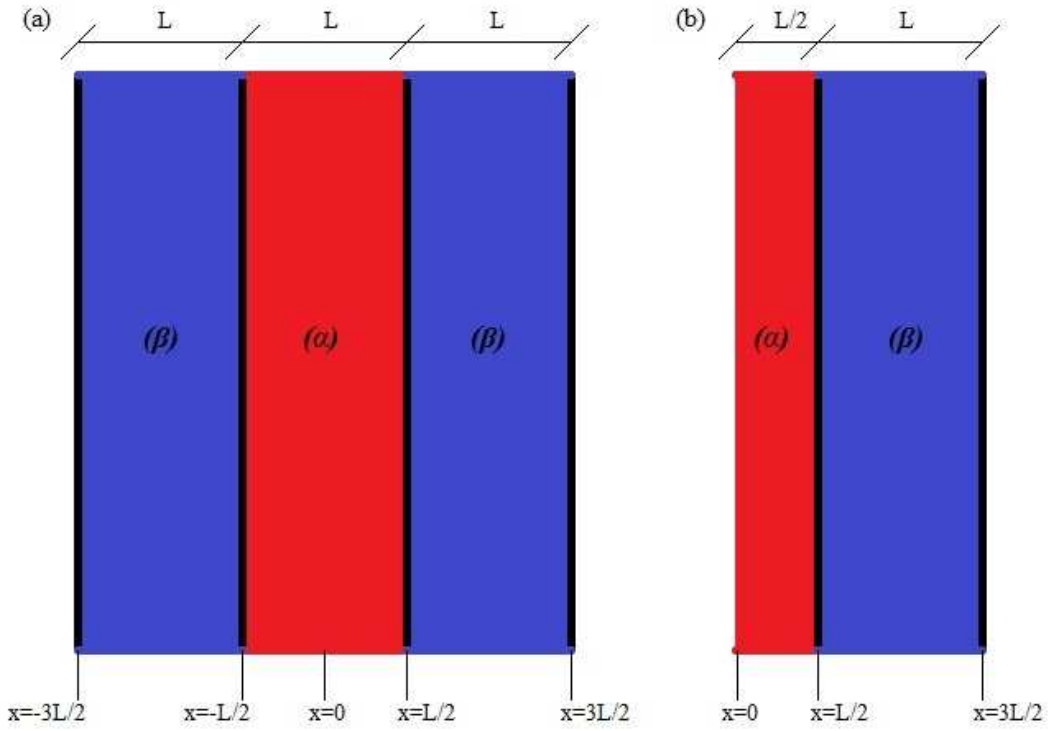

Figure 1 Schematic of (a) the entire system and (b) the half-symmetric part modelled. Layer α represents Copper while β indicates Niobium, or Vanadium **[34]**.

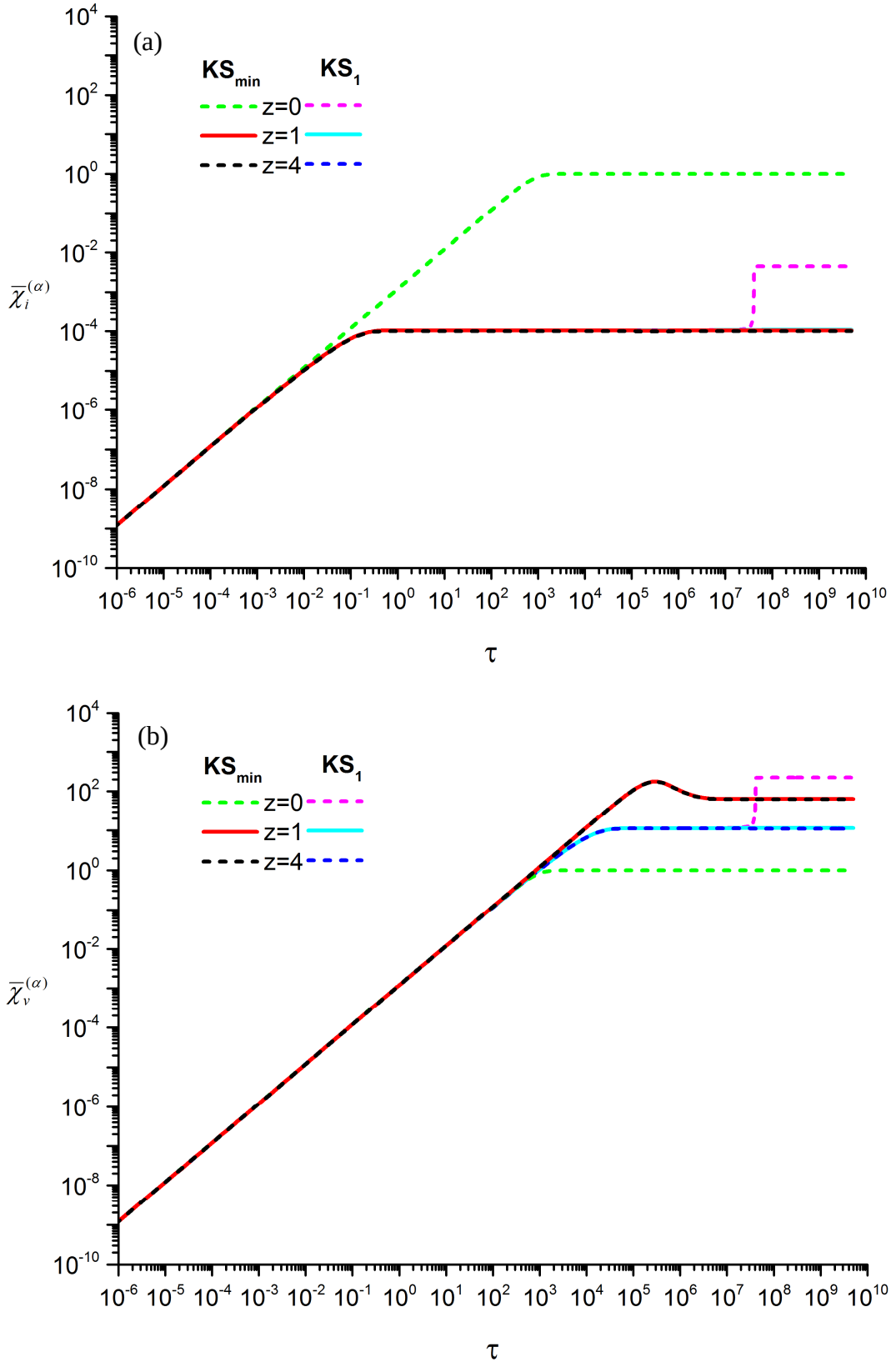

Figure 2 Temporal profiles of average (a) SIA and (b) vacancy concentration in Cu layer of Cu/Nb system for different values of parameter z .

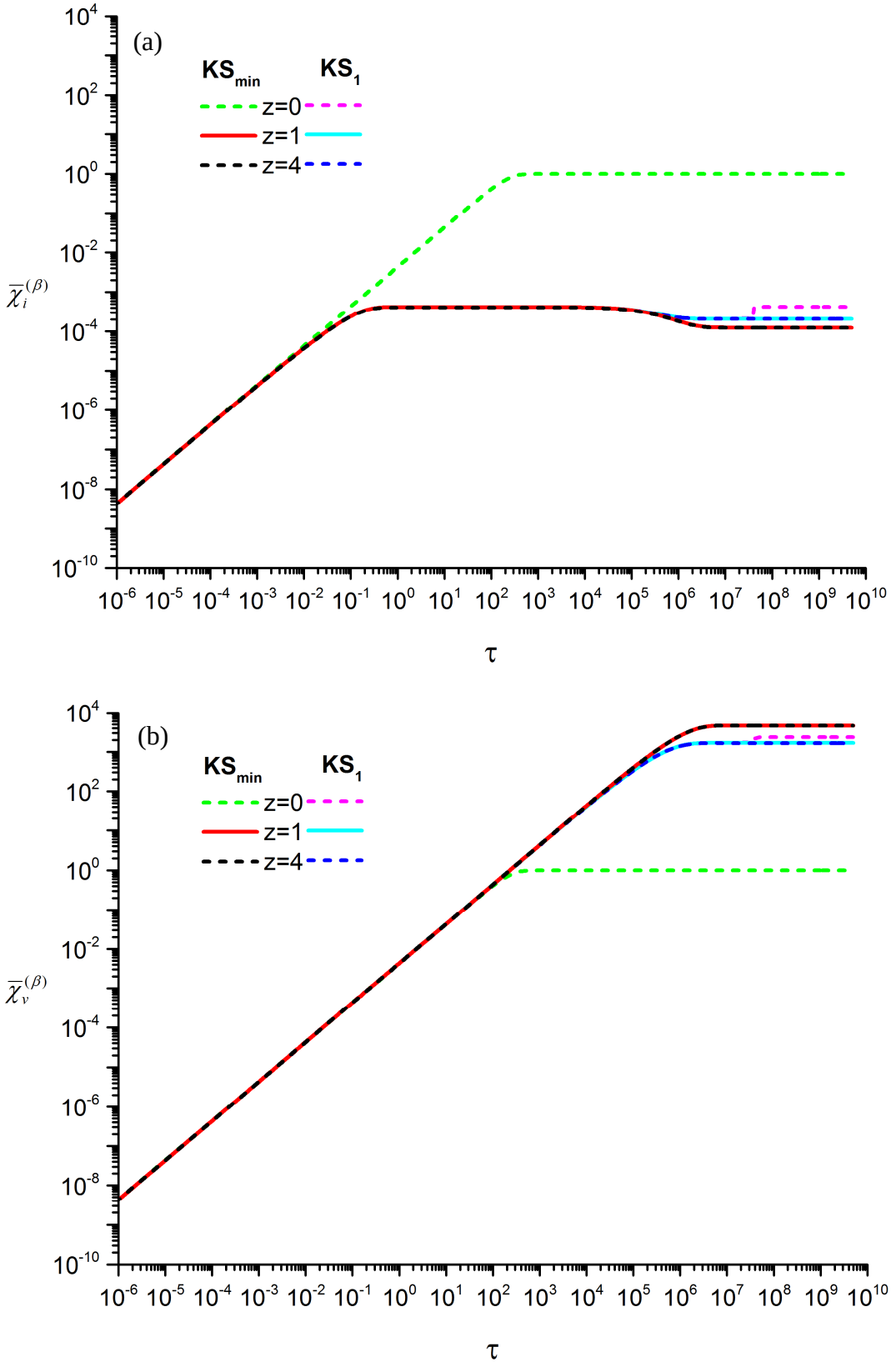

Figure 3 Temporal profiles of average (a) SIA and (b) vacancy concentration in Nb layer of Cu/Nb system for different values of parameter z .

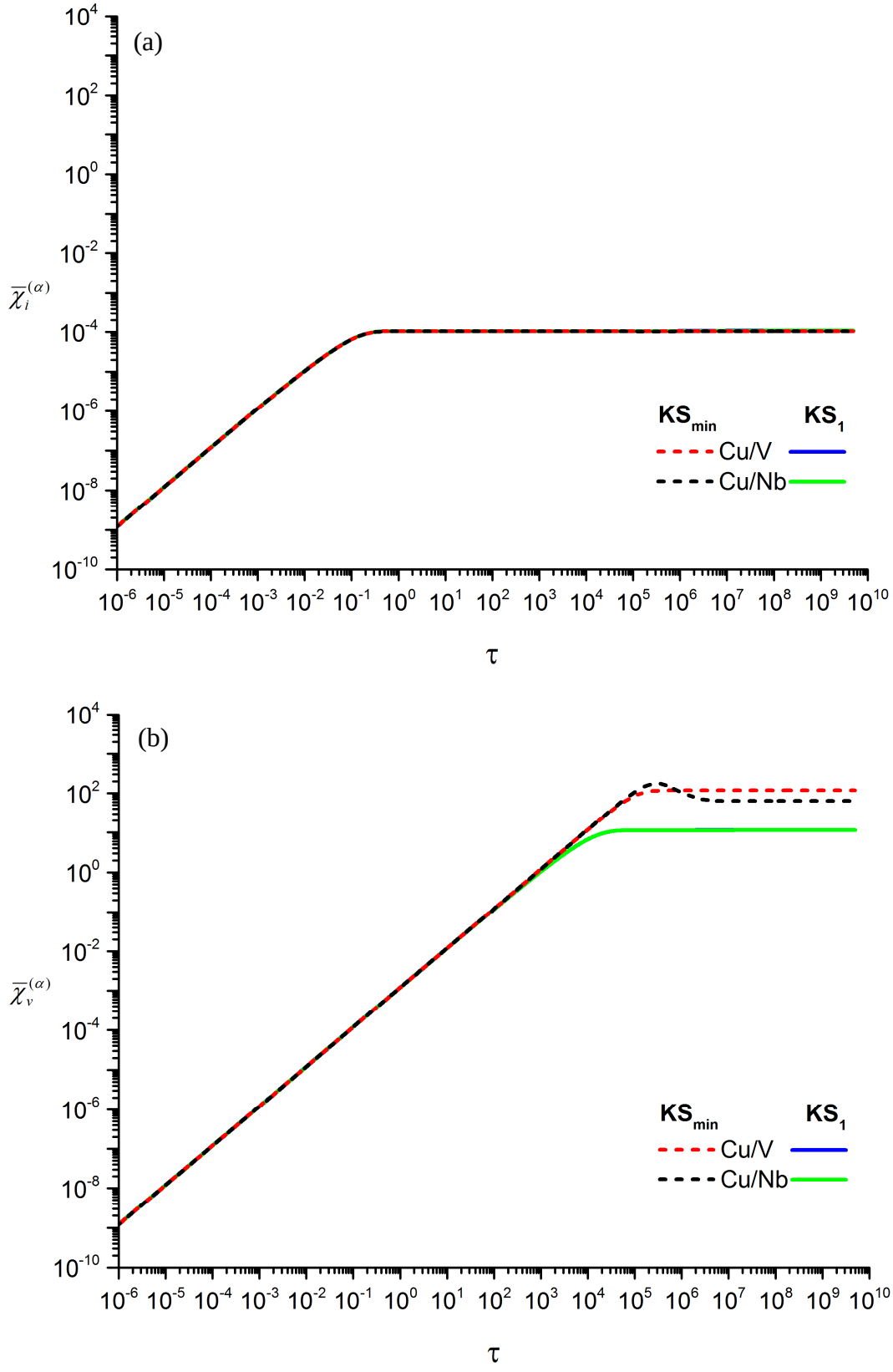

Figure 4 Temporal profiles of average (a) SIA and (b) vacancy concentration in layer α ($z = 1$).

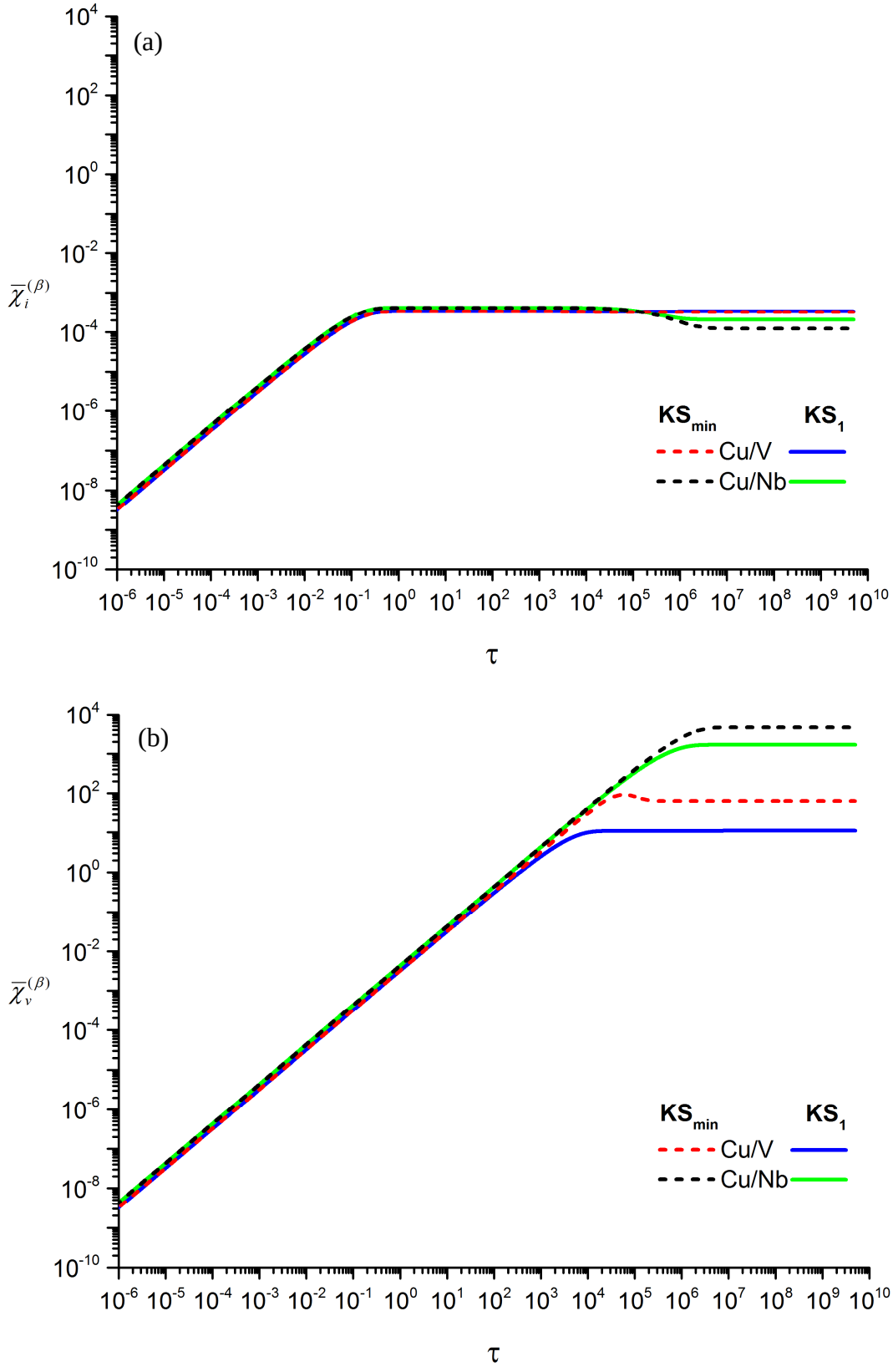

Figure 5 Temporal profiles of average (a) SIA and (b) vacancy concentration in layer β ($z = 1$).

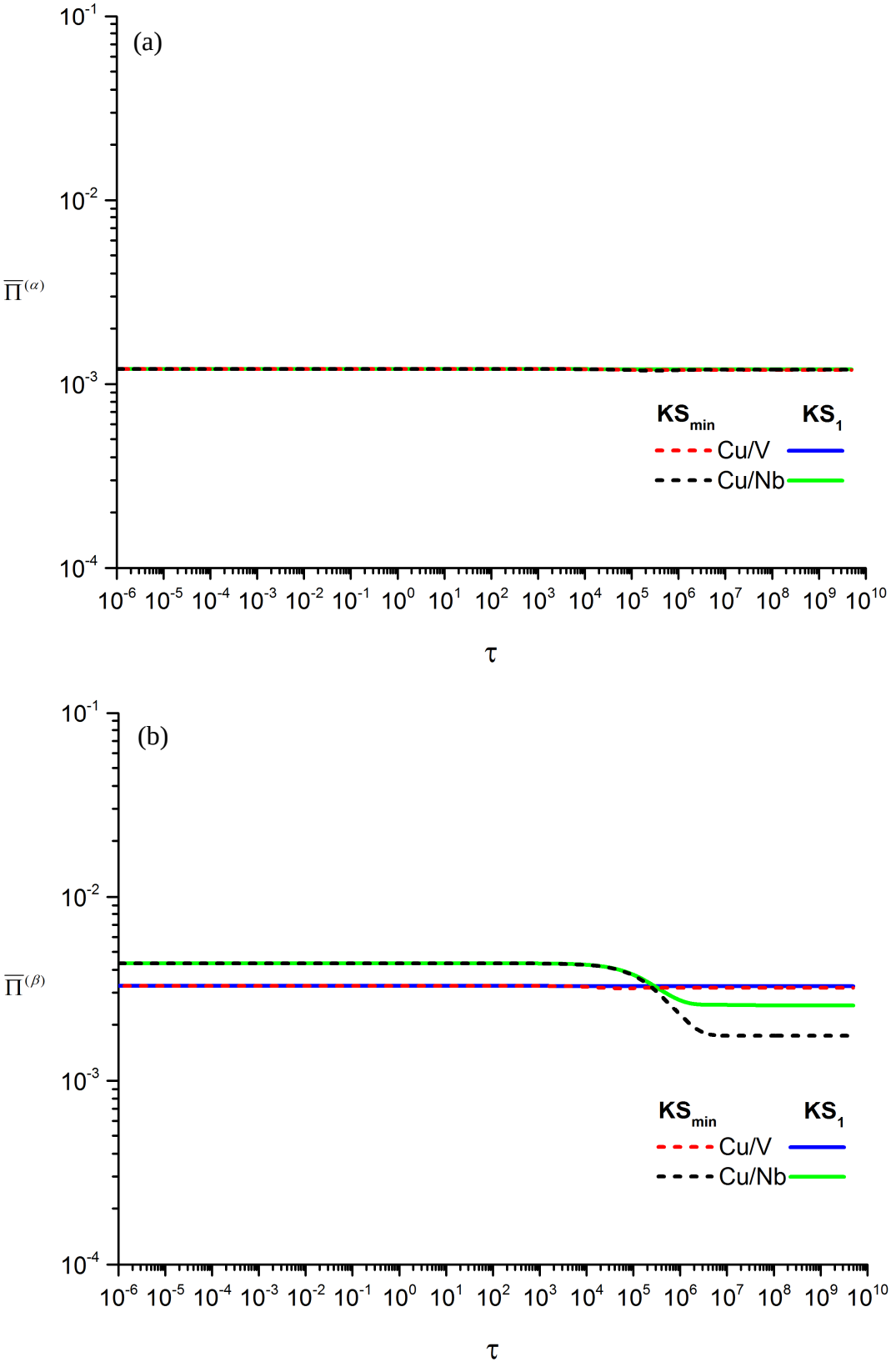

Figure 6 Temporal profiles of average point-defect net-production rate in (a) layer α and (b) layer β ($z=1$).

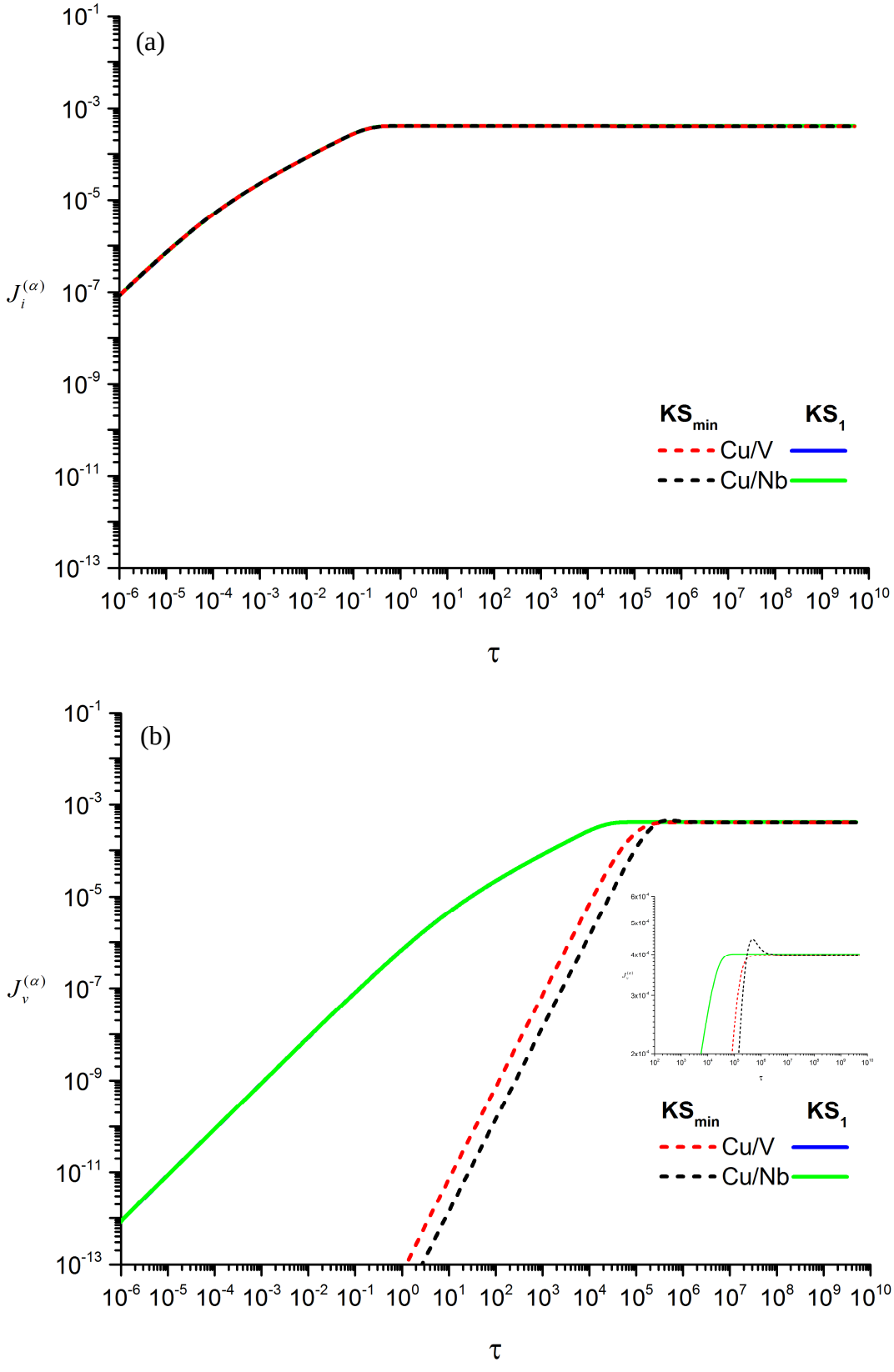

Figure 7 Temporal profiles of (a) SIA and (b) vacancy flux from layer α to the interface between metals α and β ($z = 1$).

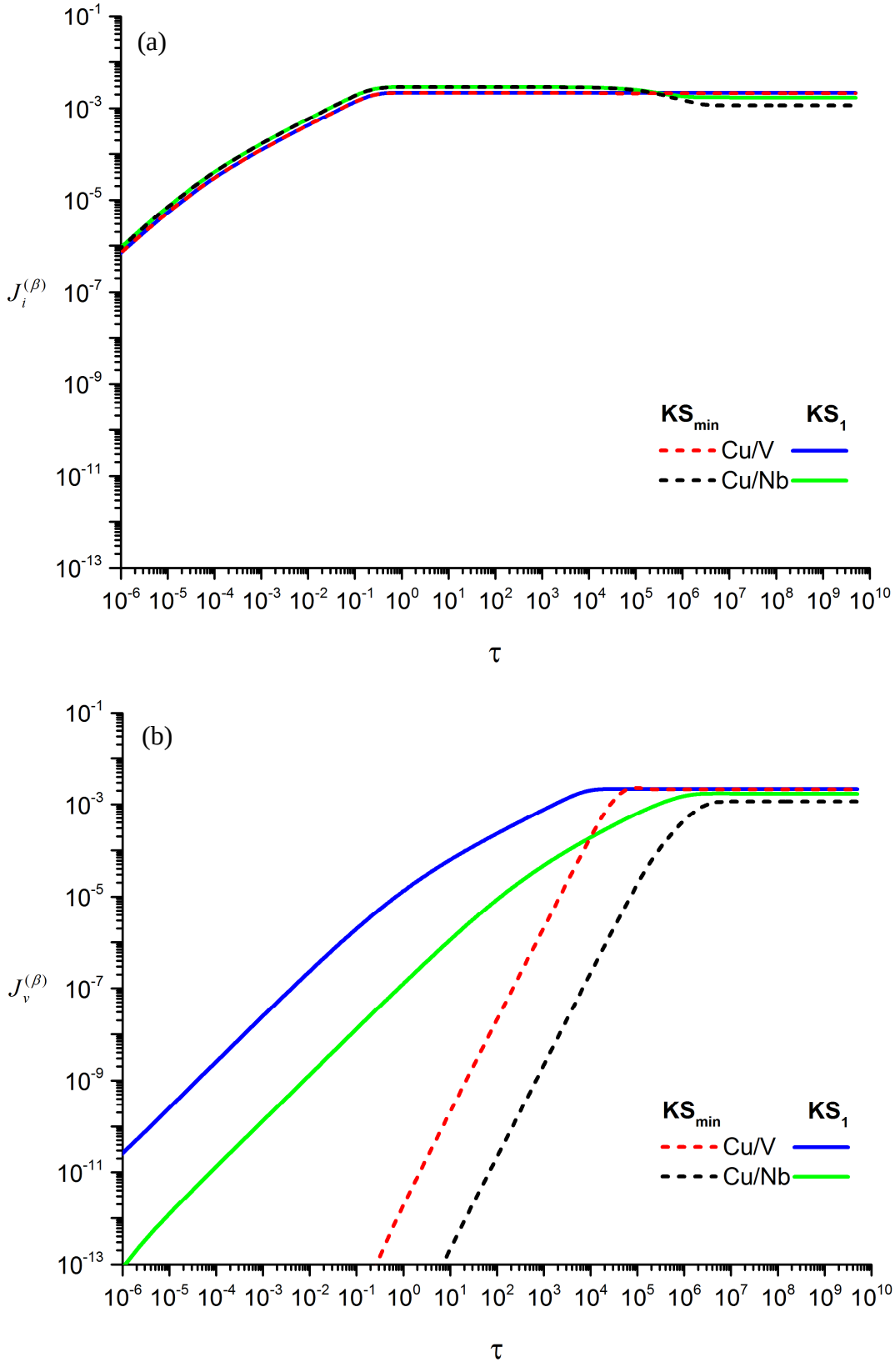

Figure 8 Temporal profiles of (a) SIA and (b) vacancy flux from layer β to the interface between metals α and β ($z = 1$).

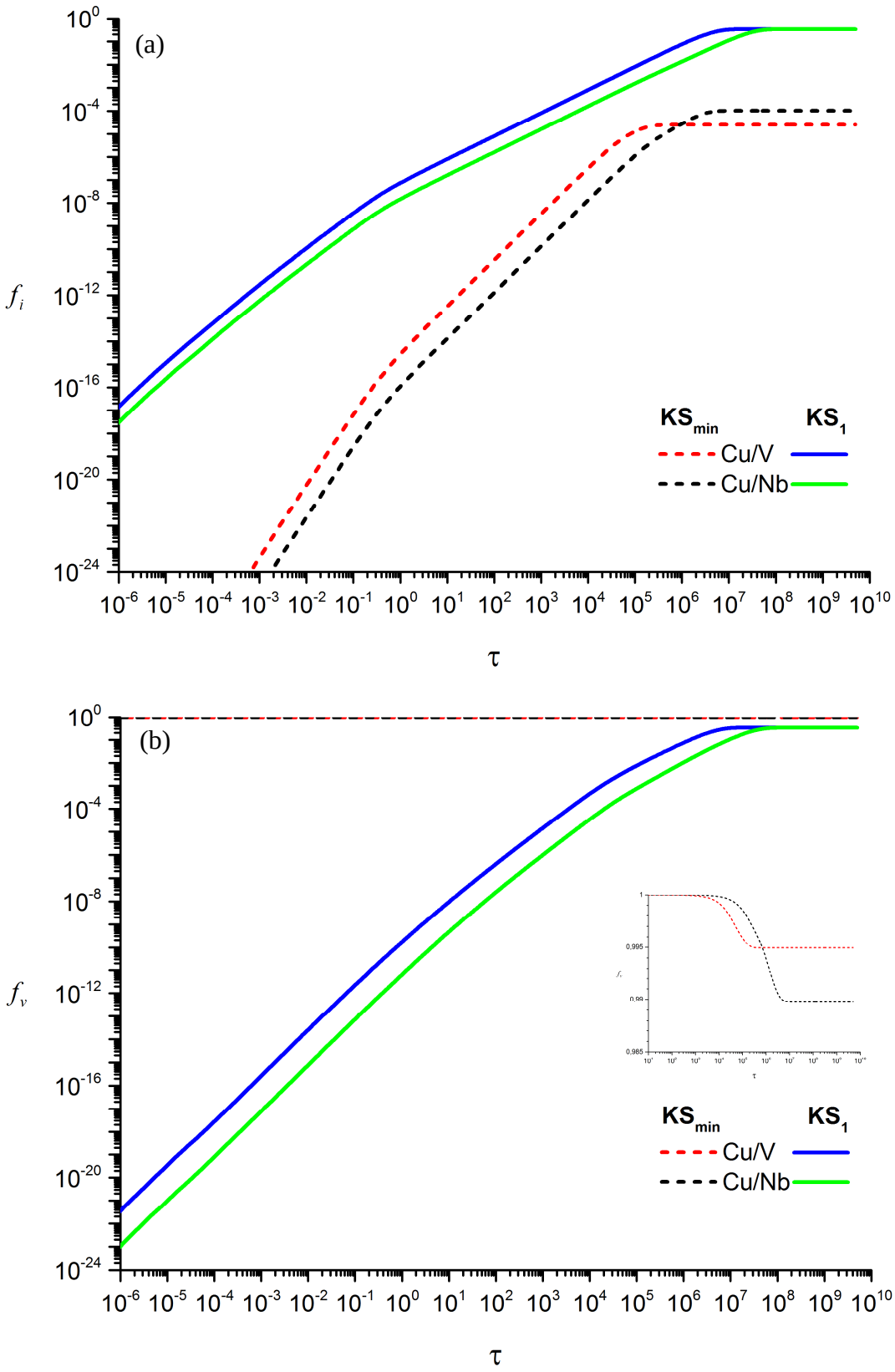

Figure 9 Temporal profiles of (a) SIA and (b) vacancy trap occupation probability at the interface between metals α and β ($z = 1$).